20th IMEKO TC4 International Symposium and
18th International Workshop on ADC Modelling and Testing
Research on Electric and Electronic Measurement for the Economic Upturn
Benevento, Italy, September 15-17, 2014

Haptic Guidance in Urban Search and Rescue Scenarios with Reduced Visibility

Stefano Scheggi[1] and Gionata Salvietti[2]

[1]*Dept. of Information Engineering and Mathematics, University of Siena, Via Roma 56, 53100 Siena*
[2]*Dept. of Advanced Robotics, Istituto Italiano di Tecnologia, Via Morego 30, 16163 Genova*

***Abstract* – The use of robots in Urban Search and Rescue (USAR) has been widely studied in the last two decades. This scenario offers a unique opportunity to investigate Human Robot Interaction (HRI) in unstructured environments. In this paper, we present a possible paradigm of communication between human and robot based on haptic guidance. In particular, we developed a HRI framework in which the human agent is guided by a robot through a vibrating bracelet. The robot has on-board the necessary sensors to localize itself on a map or to build a new map in case of debris or collapsed walls. Moreover, the robot can localize the human position using a RGB-D camera (e.g., the kinect sensor) and generate commands for the haptic guidance. This approach could be particularly suited in case of reduced visibility.**

I. INTRODUCTION

Urban Search and Rescue (USAR) requires high-level capabilities only human operators are currently capable of providing. At the same time, robots can bring the advantage of the safety and efficiency of automated tasks [1]. Typically, in USAR applications an heterogeneous group of agents (humans, robots, static and mobile sensors) enter a building and disperse, while following gradients of temperature and concentration of toxins, and looking for immobile humans [2]. The way humans and robots interact during USAR can vary significantly according to robot types and applications [3]. The robot platforms for USAR differ in terms of size, type of mobility (wheels, tracks, or combination), and ruggedness. The applications range from simple mobile sensor to operative robots able to remove debris and manipulate objects. However, even thought the capability of a robot to guide a human has been investigated in literature [4, 5], few applications are related to USAR.

In this work, we investigate how a robot can guide a human agent using a vibrotactile bracelet in a reduced visibility scenario. We supposed that the robot is able to compute its own path. The path can be computed localizing itself on an available map of the area or building a new map using the on-board sensors. Moreover, the final path can be selected according also to other sensors' measurements, e.g., temperature, percentage of oxygen, etc.. The robot is also able to track the position of the human agent using a dedicated sensor. In this preliminary phase, we used a RGB-D camera, the kinect sensor. Although the performance of the kinect sensor in environment where the visibility is reduced by fire smoke are not optimal [6], the use of other sensors in the proposed framework (e.g., laser scanner, IR cameras, sonar systems, radar etc.) is straightforward. We tested the effectiveness of the proposed control strategy in an indoor experimental setup. The participants were asked to follow a wheeled robot while blindfolded. A vibrotactile bracelet was used to guide the agent. In the scenario we envisaged, in fact, the human agent enter in the interested area wearing the bracelet and follows the robot thanks to the haptic signals displayed by the bracelet.

The rest of the paper is organized as follows. In Section II, robot localization issues are briefly recalled. In Section III the algorithm for human-robot formation control is detailed. Section IV deals with the generation of the haptic feedback necessary for the guidance. Finally, Section V reports the main results obtained, while in Section VI conclusion and future work are outlined.

II. ROBOT LOCALIZATION

Although a map of the environment can be usually available, a disaster may change the configuration of the environment itself. As a consequence, the robot must be able to learn the map of its environment and to localize itself with respect to this map. This problem is known as Simultaneous Localization and Mapping (SLAM) problem. The difficulty of this problem consists in the fact that to move precisely, a mobile robot must have an accurate environment map; however, to build an accurate map, the mobile robot's sensing locations must be known precisely.

The SLAM problem has been extensively studied in the last decades on mobile robots in 2-D indoor environment [7] and fully 3-D outdoor environments [8]. Concerning the latter, a possible localization strategy consists in fusing the data acquired by a laser scanner with the odometry of the robot estimated using the wheels encoders. Once the vehicle poses (and related 3-D point clouds) are formed, odometry provides dead-reckoned transformations between them. These information can be used in augmenting a Delayed State Extended Kalman Filter (EKF) with new vehicle poses.

ISBN-14: 978-92-990073-2-7

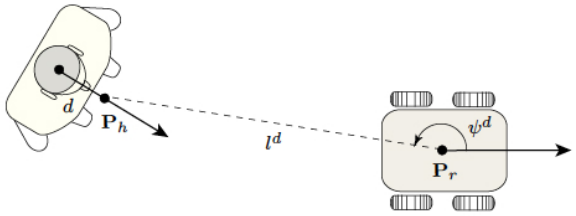

Fig. 1. Human-robot formation. l^d *and* ψ^d *represent the desired distance and orientation between the human and robot, respectively.*

Recently, there has been an increasing interest in the development of autonomous capabilities for Micro Aerial Vehicles (MAVs). The main motivation consists in the high maneuverability of MAVs which allows the achievement of more sophisticated robotics tasks. Unfortunately, the computational power of aerial vehicles is more constrained than with mobile robots. Moreover, laser scanners are too heavy for MAVs and have a limited field of view and GPS localization may suffer of accuracy issues and indoor signal reception. As a consequence, cameras and inertial sensors can be considered the only available solutions for such limited weight and calculation power. Considering the limited weight, power and computation budget on MAVs, algorithms which rely on cameras represent an appropriate solution [9], [10].

III. HUMAN-ROBOT FORMATION

In what follows, we will consider a single grounded robot which guides the human towards a desired target position. Consider a mobile robot modeled as,

$$\dot{x} = v\cos\theta, \qquad \dot{y} = v\sin\theta, \qquad \dot{\theta} = \omega,$$

where $\mathbf{R} = (x,\, y,\, \theta)^T \in \mathbb{R}^2 \times \mathbb{S}^1$ is the pose of the robot, $\overline{\mathbf{R}} = (x(0),\, y(0),\, \theta(0))^T$ the initial position and heading, and $(v,\, \omega)^T$ the control input (v represents the robot linear velocity, while ω is its angular velocity). We denote by $\mathbf{P} = (x(t),\, y(t))^T$ the position of the robot at time t.

Once the robot has built the current map of the environment, we can use such information to plan a global trajectory from the current pose to a desired one. A two level approach can be used. The first one, is based on a global view of the environment and computes a trajectory according to fixed obstacles. The second level exploits the available on-board sensors to detect dynamic obstacles and to update the trajectory, minimizing the probability of collision. In the proposed scenario, we assume that the tangent to the planned trajectory is well defined at each point, and that its curvature is known.

Given a desired trajectory, if the mobile robot $\mathbf{R}_r$ is moving with linear velocity $v_r \neq 0$, then the angular velocity ω_r that allows the robot to follow the path, assuming that the initial robot configuration is not far from the desired path, is reported in [11].

In our scenario the human should always be able to freely choose his/her linear velocity. However, in order to be driven by the robot $\mathbf{R}_r$ to the target position, his/her angular velocity should be suitably regulated. On the other side, the robot should change its linear velocity accordingly to that of the user, while its angular velocity ω_r depends on the specific trajectory as described above. The proposed human-robot formation control has been obtained from [12] which focused on formation of robots.

Such a choice was motivated by recent studies [13] which have shown a close relationship between the shape of human locomotor paths in goal-directed movements, and the simplified kinematic model of a wheeled mobile robot. Thus, nonholonomic constraints similar to those of mobile robots seem to be at work when a human is walking. As a consequence, assuming that the human is moving with linear velocity v_h and the robot is rotating with angular velocity ω_r, the human-robot formation control which allows to maintain the formation specified by a desired distance l^d and orientation ψ^d is,

$$\begin{bmatrix} \omega_h \\ v_r \end{bmatrix} = (\mathbf{G}^*)^{-1}\Big(\mathbf{q}^* - \mathbf{F}^* \begin{bmatrix} v_h \\ \omega_r \end{bmatrix}\Big), \tag{1}$$

being,

$$\mathbf{G}^* = \begin{bmatrix} (d/l)\cos\gamma & (\sin\psi)/l \\ d\sin\gamma & -\cos\psi \end{bmatrix}, \quad \mathbf{q}^* = \begin{bmatrix} k_2(\psi^d - \psi) \\ k_1(l^d - l) \end{bmatrix},$$

$$\mathbf{F}^* = \begin{bmatrix} -(\sin\gamma)/l & -1 \\ \cos\gamma & 0 \end{bmatrix},$$

$\beta = \theta_r - \theta_h$ is the relative bearing of the human and the robot, $\gamma = \beta + \psi$, d is the offset to an off-axis reference point $\mathbf{P}_h$ on the human and k_1, k_2 are positive control gains.

Suppose that the robot estimates the human motion using an onboard sensor with limited field of view. Since the formation parameters are fixed with respect to the robot, then a proper choice of l^d and ψ^d allows to always maintain the human inside the sensor's field of view, maximizing the visibility of the user.

Note that it is not trivial to impose a desired angular velocity ω_h to a human. In the next section we will show how we can use haptic feedback to address this challenging problem.

IV. HAPTIC GUIDANCE

A. Description of the haptic bracelet

The following key points were instrumental in the design of the proposed haptic interface:

- vibration is best on hairy skin and in bony areas [14], in particular, wrists and spine are generally preferred for detecting vibrations, with arms next in line [15];

- movement can decrease detection rate and increases response time of particular body areas; for example, walking affects lower body sites the most [15].

Following these considerations, we designed a vibrotactile bracelet placed in the forearm and consisted of three cylindrical vibro-motors, L (left), C (center) and R (right). A bracelet shape with three vibrating motors circling the forearm ensures sufficient distance between the motors while covering a minimal forearm area (the minimal distance between two stimuli to be differentiated is about 35 mm on the forearms [16, 14]).

Since the haptic feedback will give the human information about her/his angular velocities, two vibrating motors will be used to independently warn the user. However, since in real scenarios the maximum robot velocities are very limited, a third motor has been used to warn the human if he/she is too close to the robot.

Concerning the bracelet, the three cylindrical vibromotors are independently controlled via an external PC using the Bluetooth communication protocol (see Fig. 2). The communication is realized with a RN42 Bluetooth module connected to an Arduino mini pro 3.3V with a baud rate of 9600. An Atmega 328 micro-controller installed on the Arduino board is used to independently control the vibration amplitude of each motor. Three Precision Microdrives 303-100 Pico Vibe 3.2 mm vibration motors were placed into three fabric pockets on the external surface of the bracelet with shafts aligned with the elbow bone (see Fig. 2). The motors have a vibration frequency range of 100-280 Hz (the maximal sensitivity is achieved around 200 Hz-300 Hz [17]) and typical normalized amplitude of 0.6 g. The width of the wristband is about 60 mm.

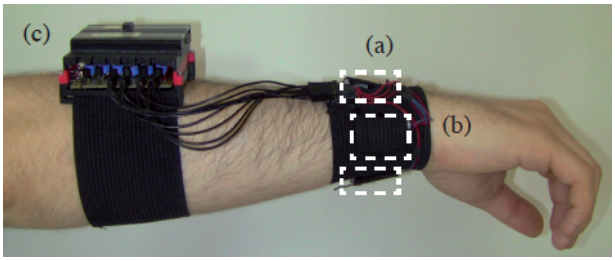

Fig. 2. The vibrotactile bracelet is equipped with three vibrating motors (a), attached to an elastic wristband (b). The three motors are disposed equidistantly in order to improve the vibrotactile perception. The Li-Ion battery and the Arduino board are in (c).

B. *Haptic feedback generation*

In order to not overload the tactile channel, a simple on/off mechanism was adopted. When a motor is engaged, it vibrates at a frequency of 250 Hz in order to achieve the maximal sensitivity. Note that all the motors have the same vibration frequency and /or amplitude.

Let $f_j(t)$ the vibration frequency of motor $j \in \{L, C, R\}$ at time t and let $\omega_h(t)$ the human angular velocity at time t and $\omega_h^*(t)$ the human angular velocity computed by the controller in (1) ($\omega_h^*(t)$ represents the angular velocity that the user should have at time $t + \Delta T$ in order to properly follow the robot, where ΔT is the discrete time step). A common hypothesis in several tracking algorithms presented in literature is that the motion characteristics of an object change very little between two subsequent frames, thus we assume that the human motion is constant between two consecutive frames, i.e., $\omega_h(t + \Delta T) = \omega_h(t)$.

As far as the angular velocity of the human is concerned, the proposed approach consists in sending a proper vibrotactile signal if the angular velocity $\omega_h^*(t)$ computed by the controller differs from the user's angular velocity $\omega_h(t + \Delta T)$ more than a given threshold $\alpha \in \mathbb{R}^+$,

$$f_L(t) = \begin{cases} 250\,\text{Hz}, & \text{if } \omega_h^*(t) - \omega_h(t + \Delta T) > \alpha, \\ 0\,\text{Hz}, & \text{otherwise}, \end{cases} \tag{2}$$

$$f_R(t) = \begin{cases} 250\,\text{Hz}, & \text{if } \omega_h^*(t) - \omega_h(t + \Delta T) < -\alpha, \\ 0\,\text{Hz}, & \text{otherwise}. \end{cases} \tag{3}$$

Since we have assumed that $\omega_h(t + \Delta T) = \omega_h(t)$, the proposed approach in (2)-(3) corrects the angular velocity of the user at time $t + \Delta T$ using the angular velocity of the human at time t and the output of the controller at time t.

Since in real world scenarios the maximal robot velocities are limited it may happen that if the human moves too fast, $v_r(t) > V_r$, where $V_r \in \mathbb{R}^+$ represents the maximal linear velocity of the robot. In this case, the robot is unable to maintain the formation. As a consequence, a proper signal is sent to the central motor to warn the human if he/she is too close to the robot. Let $\delta \in \mathbb{R}^+$ the minimal human-robot distance,

$$f_C(t) = \begin{cases} 250\,\text{Hz}, & \text{if } \|\mathbf{P}_r(t) - \mathbf{P}_h(t)\| < \delta, \\ 0\,\text{Hz}, & \text{otherwise}. \end{cases} \tag{4}$$

In order to reduce the *aftereffect* problem (vibration effects usually persist after the end of the stimulation), we displayed a periodic vibrational pattern with period 2τ instead of a continuous signal. The vibration period was determined both by mechanical limitation of the proposed motors and by pilot studies conducted on a group of subjects in order to asses which interval they preferred. Moreover, to keep the signals recognition as simple as possible,

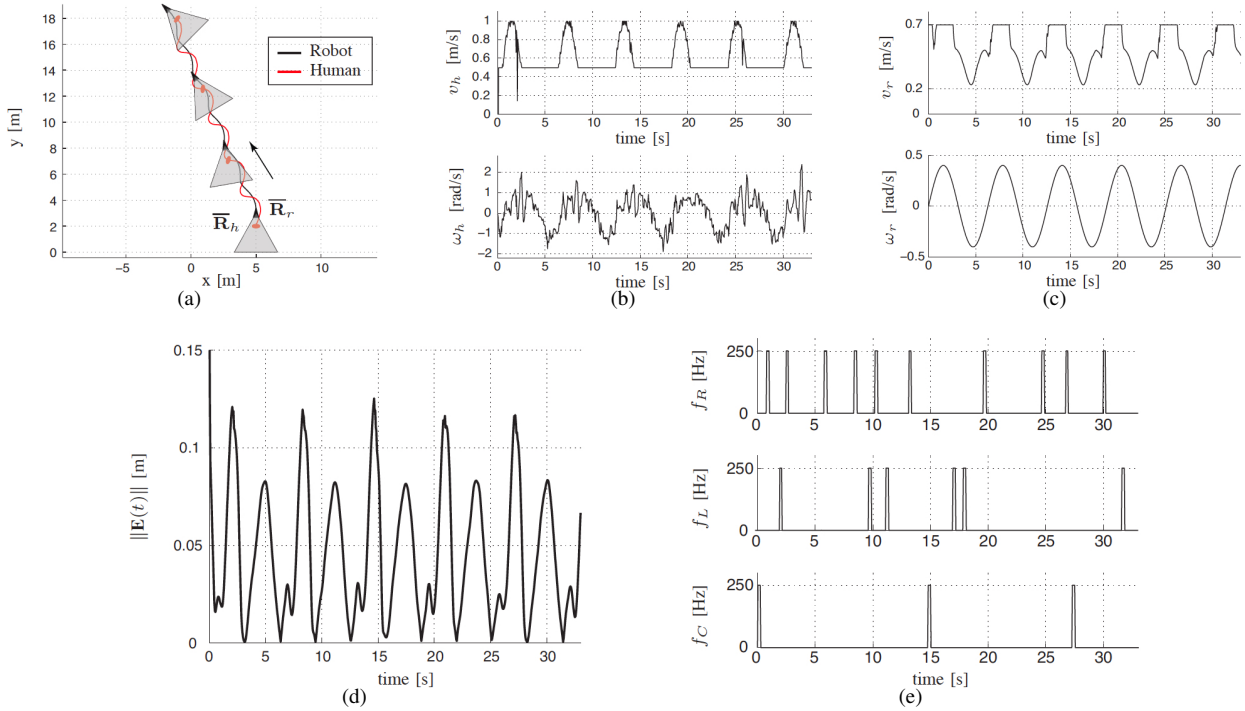

Fig. 3. Simulation results. *(a) Trajectory of the robot (black), the human (red) and related camera's field of view (shaded); (b), (c), linear and angular velocities of the human* $(v_h, \omega_h)^T$ *and of the robot* $(v_r, \omega_r)^T$*, respectively; (d) time evolution of the Euclidean norm of the formation error* $\boldsymbol{E} = (E_x,\, E_y)^T$*; (e) vibrational frequencies of the right, left and central motor of the bracelet.*

we did not consider superpositions of two signals. In case of a combination of stimuli, we alternated the two patterns. Note that in this case the second signal is shifted of half the signal period.

V. RESULTS

A. Numerical simulations

A sinusoidal trajectory has been considered to evaluate the haptic feedback generation (see Sect. B.) when the user continuously changes his/her direction. The initial conditions of the robot and the human are $\overline{\mathbf{R}}_r = (5, 3, \pi/2)^T$ and $\overline{\mathbf{R}}_h = (5, 2, \pi/2)^T$, respectively, with formation parameters $l^d = 1.2$ m, $\psi^d = \pi$ rad and $d = 0.1$ m. The control gains are $k_1 = k_2 = 10$ and the parameters for the haptic bracelet, $\delta = 1.1$ m and $\alpha = 0.5$ rad/s. We assumed that the camera's field of view has an horizontal aperture of 58 deg and maximal range of 3 m. The maximal linear velocity of the robot is $V_r = 0.7$ m/s.

In the simulation, we assumed that the user always reacts correctly to the haptic feedback and we modeled the human's angular velocity as,

$$\omega_h(t+\Delta T) = \begin{cases} \omega_h(t) + \pi/6 + z_\omega(t) & \text{if } f_L(t) \neq 0 \text{ Hz}, \\ \omega_h(t) - \pi/6 + z_\omega(t) & \text{if } f_R(t) \neq 0 \text{ Hz}, \\ \omega_h(t) + z_\omega(t) & \text{otherwise}, \end{cases}$$

where $z_\omega \sim \mathcal{N}(0,\, 10^{-2})$, i.e., z_ω is a zero-mean white Gaussian noise with variance 10^{-2} (a change in the angular velocity of about $\pi/6$ rad/s when the haptic feedback is provided to the user, was motivated by simple physical considerations). The linear velocity of the human was modeled as,

$$v_h(t+\Delta T) = \begin{cases} v_h(t) - 0.2 + z_v(t) & \text{if } f_C(t) \neq 0 \text{ Hz}, \\ h(t) + z_v(t) & \text{otherwise}, \end{cases}$$

where $z_v \sim \mathcal{N}(0,\, 5 \times 10^{-2})$ and

$$h(t) = \frac{(\sin t - 0.5)(\mathrm{sgn}(\sin t - 0.5) + 1)}{2} + 0.5,$$

being $\mathrm{sgn}(\cdot)$ the sign function. The human's velocity is represented by a sinusoidal function with maximal value 1 m/s and minimal value 0.5 m/s. When the distance between the user and the robot is less than δ, the central motor of the bracelet is engaged and the user decreases his/her linear velocity of about 0.2 m/s.

Fig. 3(a) reports the trajectory of the robot (black) and of the human (red) together with camera's field of view (shaded), Fig. 3(b)-(c) the linear and angular velocities $(v_h,\, \omega_h)^T$, $(v_r,\, \omega_r)^T$ of the two agents, and Fig. 3(d) the time evolution of the Euclidean norm of the formation error,

$$\mathbf{E}(t) = (E_x(t), E_y(t))^T \triangleq \mathbf{P}_h(t) - l^d\,(\cos\psi^d,\, \sin\psi^d)^T.$$

Finally, Fig. 3(e) shows the (simulated) vibrational frequencies of the right, left and central motor of the haptic bracelet.

B. Experiments

The effectiveness and robustness of control strategy (1) has been tested in an indoor environment using a Pioneer P3AT robot (with maximal linear velocity of 0.7 m/s) equipped with a backward facing Microsoft's Kinect camera. Six healthy subjects (age range 23-30, all males and right-handed) were involved in our tests. All subjects were blindfolded and instructed to move accordingly to the haptic feedback, but no instructions were given about their linear and/or angular velocities. Two different trajectories were considered for the robot in order to test the haptic feedback when the user continuously changes his/her direction (see Fig. 4(a)). Each subject performed 4 trials: 2 trials with trajectory A and 2 trials with trajectory B in a randomized order.
The human motion was computed using a custom visual tracking algorithm which run at an average frame rate of 17 fps on a laptop with 8 GB RAM, 2.9 GHz Intel i5 CPU and NVIDIA GeForce GT 540M (2GB DDR3) graphic card. Due to the motors' actuation time of the mobile robot, the human-robot's velocities were computed every 0.2 sec. and sent to the robot via the TCP/IP protocol. Regarding the formation parameters, we set $l^d = 2.3$ m and $\psi^d = \pi$, $k_1 = k_2 = 5$, $d = 0.1$ m, $\alpha = 0.8$ rad/s and $\delta = l^d - 0.2$ m.

The initial and final displacements of the robot and the human are reported in Fig. 4(a). Fig. 4(b) shows the time evolution of the norm of the formation error $\mathbf{E}(t) = (E_x(t),\, E_y(t))^T$ of the fourth subject. Fig. 4(c) shows the mean (and the standard deviation) of the formation error for each trial $\mathbf{E}^i(t)$, $i = 1, 2, \ldots, 24$. In blue is reported the first subject who did not participate in the evaluation of the haptic device. As we can notice from Fig. 4(c), the mean of the formation error is always smaller than 0.9 m. Moreover, although the first user never tried the haptic wristband before, he was able to correctly recognize the haptic stimuli and follow the robot.

Results showed the functionality of the proposed approach. The mean of the formation error $\mathbf{E}^i(t)$ among all the trials, is 0.52 m with a standard deviation of 0.16 m. In this regard, the robot trajectories represent a sort of worst case due to the continuos change of the human direction.

VI. CONCLUSION AND FUTURE WORK

In this paper we have presented a new haptic paradigm for the guidance of a human in an unknown environment with a mobile robot. The subject is free to decide his/her own gait and a warning vibrational signal is generated by the wrist-worn haptic bracelet only when a large deviation with respect to the planned route occurs. The proposed haptic guidance framework could be suitable in USAR scenario where the robot can guide the operator in the disaster area. Real world experiments revealed the effectiveness of the proposed approach. We are planning to use different sensors to track the human motion in order to test also the performance of the proposed approach in smoky environments.

VII. *

References

[1] Chipalkatty, R., Daepp, H., Egerstedt, M., and Book, W. *Human-in-the-loop: MPC for shared control of a quadruped rescue robot.* In Intelligent Robots and Systems (IROS), IEEE/RSJ International Conference on (pp. 4556-4561), 2011.

[2] G. Kantor, et al. *Distributed search and rescue with robot and sensor teams*, 2003.

[3] Murphy, Robin Roberson. *Human-robot interaction in rescue robotics*, Systems, Man, and Cybernetics, Part C: Applications and Reviews, IEEE Transactions on, vol 34, pp 138–153, 2004.

[4] Philippsen, Roland, and Roland Siegwart. *Smooth and efficient obstacle avoidance for a tour guide robot*, In Proc. IEEE Int. Conf. on Robotics and Automation, 2003.

[5] S. Scheggi, M. Aggravi, F. Morbidi, D. Prattichizzo, *Cooperative human-robot haptic navigation*, In Proc. IEEE Int. Conf. on Robotics and Automation, Hong Kong, China, 2014.

[6] Starr, Joseph W., and B. Y. Lattimer. *Evaluation of Navigation Sensors in Fire Smoke Environments*, Fire Technology, 1-23, 2012.

[7] D. Hahnel, W. Burgard, D. Fox and S. Thrun. *An efficient FastSLAM algorithm for generating maps of large-scale cyclic environments from raw laser range measurements.* In Proc. IEEE/RSJ Int. Conf. on Intelligent Robots and Systems, pp. 206-211, 2003.

[8] D. M. Cole and P. M. Newman. *Using laser range data for 3D SLAM in outdoor environments.* In Proc. IEEE Int. Conf. on Robotics and Automation, pp. 1556-1563, 2006.

[9] G. H. Lee, F. Fraundorfer and M. Pollefeys. *MAV visual SLAM with plane constraint.* In Proc. IEEE Int. Conf. on Robotics and Automation, pp. 3139-3144, 2011.

[10] L. Doitsidis, S. Weiss, A. Renzaglia, M. W. Achtelik, E. Kosmatopoulos, R. Siegwart and D. Scara-

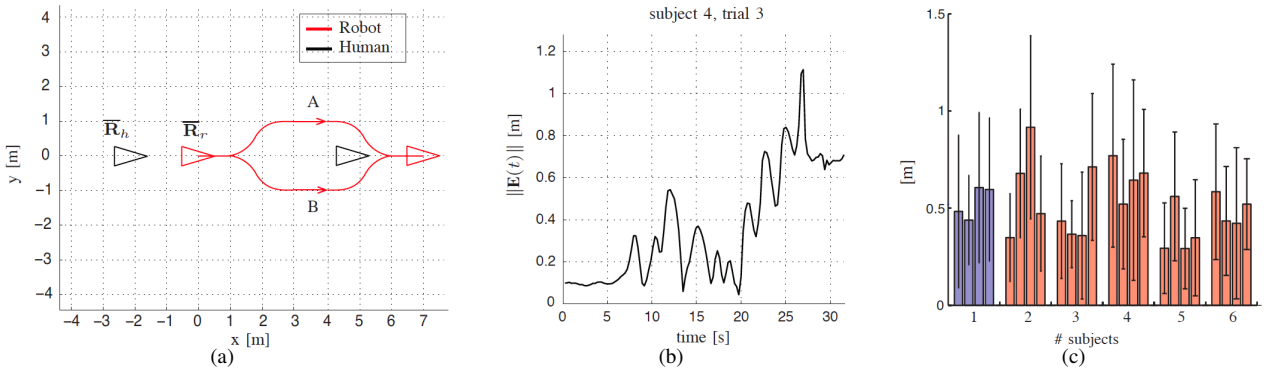

Fig. 4. Experimental results. *(a) Initial and final disposition of the robot (red) and human (black) and planned trajectories of the robot (red); (b) time evolution of the Euclidean norm of the formation error* $\boldsymbol{E}(t) = (E_x(t),\ E_y(t))^T$ *for the fourth subject; (c) mean and standard deviation of the norm of the formation error over the 24 trials for the 6 subjects.*

muzza. *Optimal surveillance coverage for teams of micro aerial vehicles in GPS-denied environments using onboard vision.* Auton. Robot., 33(1-2):173-188, 2011.

[11] D. Fontanelli, A. Giannitrapani, L. Palopoli, and D. Prattichizzo. *Unicycle steering by brakes: a passive guidance support for an assistive cart.* In Proc. IEEE Conf. Dec. Contr, pp. 2275-2280, 2013.

[12] A.K. Das, R. Fierro, V. Kumar, J.P. Ostrowski, J. Spletzer, and C.J. Taylor. *A vision-based formation control framework.* IEEE Trans. Robotic. Autom., 18(5):813–825, 2002.

[13] G. Arechavaleta, J.P. Laumond, H. Hicheur, and A. Berthoz. *On the nonholonomic nature of human locomotion.* Auton. Robot., 25(1):25-35, 2008.

[14] F. Gemperle, T. Hirsch, A. Goode, J. Pearce, D. Siewiorek, and A. Smailigic. *Wearable vibro-tactile display*, 2003. Carnegie Mellon University.

[15] I. Karuei, K.E. MacLean, Z. Foley-Fisher, R. MacKenzie, S. Koch, and M. El-Zohairy. *Detecting vibrations across the body in mobile contexts.* In Proc. Int. Conf. Human Factors Comp. Syst., pp. 3267-3276, 2011.

[16] S. Weinstein. *Intensive and extensive aspects of tactile sensitivity as a function of body part, sex, and laterality.* In Spriengfield, editor, The skin senses, pp. 195–218. Erlbaum, 1968.

[17] A. Riener. *Sensor-actuator supported implicit interaction in driver assistance systems.* In S. Hölldobler et al., editor, Ausgezeichnete Informatikdissertationen 2009, 10:221-230. Gesellschaft für Informatik, Bonn, 2010.